Oxaliplatin resistance in pancreatic ductal adenocarcinoma is non-significantly mediated by diminished drug uptake but is highly linked to a poor apoptotic response to the cytotoxic threat

HELLEN RÖTTGEN[1*], LANA THEURER[2*], TERESA PECCERELLA[3], KETAKI SANDU[1], JOHANNA WEISS[1], JÜRGEN BURHENNE[1], JOHN P. NEOPTOLEMOS[3], BEATE KÖBERLE[2] and DIRK THEILE[1]

[1]Internal Medicine IX-Department of Clinical Pharmacology and Pharmacoepidemiology, Heidelberg University, Medical Faculty Heidelberg, Heidelberg University Hospital, D-69120 Heidelberg, Germany; [2]Department of Food Chemistry and Toxicology, Karlsruhe Institute of Technology, D-76131 Karlsruhe, Germany; [3]Department of General, Visceral, and Transplantation Surgery, Heidelberg University, Medical Faculty Heidelberg, Heidelberg University Hospital, D-69120 Heidelberg, Germany

Received June 26, 2025; Accepted October 1, 2025

DOI: 10.3892/or.2025.9027

Abstract. Pancreatic ductal adenocarcinoma (PDAC) resistance to oxaliplatin is associated with diminished drug uptake and a poor molecular apoptotic response; however, the relative contribution of each of these modes of resistance remains unclear. Accordingly, PDAC cell lines (AsPC-1 and BxPC-3) and human patient-derived organoids (hPDOs; h08 and h19) were assessed in the present study, with proliferation assays, atomic absorption spectroscopy-based quantification of intracellular oxaliplatin, luminogenic caspase 3/7 assays, PCR array-based transcriptomic analysis and RNA sequencing performed to scrutinize the oxaliplatin resistance phenotype. Notably, AsPC-1 cells [half maximal inhibitory concentration (IC_{50}), 88.8±45 μM were 4.2-fold more oxaliplatin resistant than BxPC-3 cells (IC_{50}, 21±0.7 μM; P=0.02)]. In addition, when normalized to intracellular platinum levels, AsPC-1 cells remained 2.5-fold more resistant than BxPC-3 (the fold difference was decreased by 40% from 4.2-fold to 2.5-fold; P=0.21). In hPDOs, resistant h19 took up oxaliplatin 22% less efficiently than sensitive h08, and the nominal resistance difference was 3.5-fold, and it remained at 2.8-fold after controlling for drug accumulation (the fold difference was decreased by 20% from 3.5-fold to 2.8-fold; P=0.34). These findings indicated that diminished drug uptake non-significantly contributed to oxaliplatin resistance, which was in agreement with the rather minor differences in drug transporter expression levels (including *ATP7A* and *ATP7B*). Furthermore, when challenged with identical intracellular oxaliplatin levels, AsPC-1 cells exhibited delayed caspase 3/7 activity initiation, weaker induction of pro-apoptotic genes *BBC3* (1.7-fold vs. 5-fold) and *PMAIP* (2.5-fold vs. 6-fold), but stronger enhancement of anti-apoptotic *Jun* expression (7-fold vs. 3-fold) than BxPC-3 cells. Taken together, oxaliplatin resistance in PDAC models may be highly linked to a poor apoptotic response, whereas drug uptake seems to be of minor relevance.

Introduction

Despite the improvements in early detection due to better imaging, more advanced surgical techniques and individualized systemic therapies, pancreatic ductal adenocarcinoma (PDAC) remains a highly fatal type of cancer. In the last 40 years, several systemic adjuvant chemotherapy protocols have been evaluated, which have improved disease-free survival and overall survival (1,2). For example, adding oxaliplatin to standard gemcitabine therapy has been shown to be more efficacious than treatment with gemcitabine alone (3,4). At present, oxaliplatin remains one of the mainstay drugs for PDAC treatment, including in combination with folinic acid and 5-fluorouracil, or with additional irinotecan (5). The pharmacological mechanism of oxaliplatin includes cellular uptake, release of the oxalate group, and the subsequent binding of the positively charged platinum moiety to the N7 atom of the purine bases adenine and guanine, leading to cytotoxic adducts at DNA or DNA cross-links. Accordingly, oxaliplatin resistance is mechanistically related to these molecular steps (6).

In general, two basic modes can lead to oxaliplatin resistance: i) Poor oxaliplatin accumulation due to low expression of important influx transporters, such as organic cation transporters 1-3

Correspondence to: Professor Dirk Theile, Internal Medicine IX-Department of Clinical Pharmacology and Pharmacoepidemiology, Heidelberg University, Medical Faculty Heidelberg, Heidelberg University Hospital, 410 Im Neuenheimer Feld, D-69120 Heidelberg, Germany
E-mail: dirk.theile@med.uni-heidelberg.de

*Contributed equally

Abbreviations: PDAC, pancreatic ductal adenocarcinoma; hPDOs, human patient-derived organoids; IC_{50}, half maximal inhibitory concentration

Key words: oxaliplatin resistance, pancreatic ductal adenocarcinoma, drug uptake, human patient-derived organoids, AsPC-1, BxPC-3

(encoded by *SLC22A1-3*) or human copper transporter 1 (encoded by *SLC31A1*), or high expression of oxaliplatin efflux transporters, including multidrug resistance-related protein 2 (MRP2, encoded by *ABCC2*), Menkes' protein (encoded by *ATP7A*) or Wilson disease protein (encoded by *ATP7B*) (7,8). ii) An altered molecular response to the drug (6). Among the numerous molecular factors involved in unresponsiveness to oxaliplatin, alterations in the DNA damage response or cell cycle regulation seem to be of particular relevance (9). For example, expression and activity of MAPK-activated protein kinase 2 (10), TGF-β-activated kinase-1 (11), RAS oncogene family-like protein 6 isoform A (12), DNA methyltransferase 3a (13), BRCA2 (14), the HuR/Wee1 axis (15) or the hepatocyte nuclear factor 1 homeobox A/p53-binding protein 1 axis (16) have been implicated in oxaliplatin resistance in PDAC. Taken together, oxaliplatin resistance in PDAC is considered to be caused by the combined effect of poor drug uptake and an altered molecular response to the cytotoxic threat. However, there is little knowledge on which mechanism dominates. Accordingly, the present study evaluated the anti-proliferative pharmacodynamics of oxaliplatin [half maximal inhibitory concentration (IC_{50}) values] in PDAC models assessing both nominal extracellular drug concentrations and also the resulting intracellular concentrations, allowing for the quantification of the relative contribution of drug uptake to the overall resistance phenotype. At identical intracellular platinum concentrations, the kinetics of caspase 3/7 activity, and transcriptomic changes associated with DNA damage response, cell cycle regulation, inflammation and fibrosis signaling, and redox regulation were recorded. Eventually, baseline expression levels of associated genes and oxaliplatin drug transporters were evaluated.

Materials and methods

Cell lines. AsPC-1 (classical-like) and BxPC-3 (basal-like) PDAC cells were purchased from American Type Culture Collection. The cells were cultured in RPMI-1640 medium (PAN-Biotech GmbH), supplemented with 10% fetal bovine serum, 100 U/ml penicillin and 100 μg/ml streptomycin sulfate (all from Sigma-Aldrich; Merck KGaA), in 75 cm^2 flasks at 37˚C and 5% CO_2. The medium was changed twice a week and cells were passaged at ~80% confluence.

Human patient-derived organoids (hPDOs). hPDOs were obtained from patients undergoing surgical PDAC resection (with or without neoadjuvant chemotherapy) and were characterized with much detail (17). h08 is a basal-like organoid, whereas h19 is a classical-like organoid, with missense mutations in *TP53*, *BRCA1*, *SETD2*, *SPTB*, *BCORL1*, *ITPR3* and *TLE4*. Moreover, h19 harbors a frameshift deletion in *CDKN2A*, and multi-hit mutations in *SMAD4* and *BRCA2*; phenotypically, it has shown high resistance against several cytotoxic drugs (17).

Proliferation assay for PDAC cell lines. To assess the anti-proliferative pharmacodynamics of oxaliplatin, $2x10^4$ AsPC-1 cells/well or $1x10^4$ BxPC-3 cells/well were seeded into clear 96-well plates. One cell-free column served as a blank for later staining. After 24 h of cell attachment, the medium was discarded and replaced with medium containing different concentrations of cisplatin (control drug, obtained from the Heidelberg University Hospital Pharmacy as a 1 mg/ml stock) and oxaliplatin (obtained from the Heidelberg University Hospital Pharmacy as a 1 mg/ml stock) (AsPC-1, 1-1,000 μM; BxPC-3, 5-500 μM). After 4 h of exposure at 37˚C, the drug-containing medium was replaced with drug-free medium and the cells were cultured for an additional 48 h at 37˚C. Subsequently, the medium was removed and the cells were washed with PBS, after which 50 μl crystal violet was added to all wells and incubated on a shaker for 10 min at room temperature. After removal of the crystal violet solution, all wells were washed with tap water and dried at 37˚C. By adding 99.9% methanol, the cell-bound dye was dissolved, and the SpectraMax iD3 Multi-Mode Microplate Reader (Molecular Devices, LLC) was used to measure the absorbance at 555 nm.

To obtain values corresponding to the proliferation at each concentration, the mean of the blank absorption values was subtracted from all other absorption values, and values from the drug-treated cells were normalized to untreated cells (18). IC_{50} values were calculated based on a sigmoidal dose-response curve with variable slope of the log-transformed data.

Proliferation assay for hPDOs. The organoids were dissociated into single cells using TrypLE (cat. no. 12604013; Thermo Fisher Scientific, Inc.) according to the manufacturer's instructions and were dispensed through a 40-μm cell sieve (cat. no. 542040; Greiner Bio-One), before seeding 1,000 cells in 10 μl Matrigel/well into white 96-well plates. Oxaliplatin was added 72 h after plating, covering a concentration range of 50-5,000 μM. After 4 h of treatment at 37˚C, the medium was replaced with drug-free complete medium and 48 h after this, cell viability was assessed using the CellTiter-Glo 3D cell viability assay (Promega Corporation). Briefly, 50 μl CellTiter Glo 3D was added to the medium of each well, after which, the plate was placed on an orbital shaker (600 rpm) for 5 min at room temperature and incubated for a further 25 min at room temperature. Luminescence was measured using the FLUOstar OPTIMA (BMG Labtech GmbH). Luminescence values were blank-corrected and values from the drug-treated cells were normalized to untreated cells. A four-parameter log-logistic function was fitted to the drug response curve and IC_{50} values were calculated.

Evaluating total intracellular platinum concentrations

Sample preparation. To evaluate the resulting intracellular platinum concentrations after drug exposure, $1x10^6$ cells (AsPC-1 and BxPC-3) were seeded into each well of 6-well plates and cultured for 24 h at 37˚C and 5% CO_2. Subsequently, the cells were exposed to various concentrations of oxaliplatin or cisplatin (5, 10, 50, 100 and 1,000 μM) for 4 h at 37˚C; after which, the drug-containing medium was removed and the cells were washed thoroughly with PBS. HNO_3 (0.4%; 150 μl) in distilled water was then added for cell lysis and the cells were scraped from the bottom of the well. The lysate was transferred into a tube and sonicated (35 kHz) for 30 min at room temperature, followed by centrifugation at 17,000 x g for 3 min at room temperature. The supernatant above the debris pellet was transferred into a new tube and stored at -20˚C until further analysis.

Drug uptake into hPDOs was evaluated similarly. After seeding $2x10^5$ cells into the wells of 24-well plates, drug treatment, lysis, sonication and centrifugation were performed as aforementioned, and the supernatants were stored at -20˚C until platinum concentrations were analyzed.

Graphite furnace atomic absorption spectrometry. The platinum concentration of the lysates (obtained from cell lines and hPDOs) was analyzed with a PinAAcle 900Z graphite furnace atomic absorption spectrometer (PerkinElmer, Inc.). The samples were loaded into the sample cups of the autosampler, which injected 20 μl each sample into the graphite furnace. The furnace protocol consisted of 30 sec at 110˚C, 30 sec at 130˚C, 20 sec at 1,300˚C, 5 sec at 2,200˚C and 3 sec at 2,450˚C. The platinum absorbance was measured at 265.94 nm. For the calibration curve, six concentrations (25, 50, 100, 500, 1,000 and 5,000 μg/l) were aliquoted by the autosampler from respective stock solutions. To demonstrate the accuracy of the method, three samples for quality control (QC) were prepared by spiking 0.4% HNO_3 with the respective volume of platinum stock solution, leading to QC samples within the low, mid and high range of the calibration curve.

BCA assay. The protein concentration of all samples was evaluated using the Pierce BCA Protein Assay Kit (Thermo Fisher Scientific, Inc.). For the calibration curve, standard samples of bovine serum albumin (provided in the kit) in 0.1% HNO_3 at concentrations of 0, 25, 125, 250, 500, 750, 1,000, 1,500 and 2,000 μg/ml were prepared and the absorption was measured at 562 nm. The cell lysate samples were analyzed accordingly and the protein concentration was determined from the absorption via the linear equation of the calibration curve. The measured platinum concentrations of the lysates were normalized to the protein concentration of the lysates, eventually representing the total intracellular platinum concentration.

Validation of platinum drug uptake. The intracellular platinum concentration was plotted over the extracellular concentration for the two PDAC cell lines. A simple linear regression was used to determine an equation describing the uptake of each cell line treated with either cisplatin or oxaliplatin. The regression line was used to determine the necessary extracellular concentration that leads to the same intracellular platinum concentration in all cells. The uptake was validated by exposing the cells to these concentrations and analyzing the intracellular concentration again.

Caspase 3/7 assay. The enzyme activity of caspase 3/7 was analyzed at 0, 4, 8, 12, 18, 24 and 48 h after the 4-h treatment of PDAC cell lines at 37˚C with drug concentrations (AsPC-1: 150 μM cisplatin or 176 μM oxaliplatin; BxPC-3: 65 μM cisplatin or 150 μM oxaliplatin) known to result in identical total intracellular platinum concentrations using the Caspase-Glo® 3/7 kit (cat. no. G8091; Promega Corporation). Caspase 3/7 activity was additionally recorded in AsPC-1 cells 36 h after treatment. Briefly, $1.5x10^3$ cells/well were seeded into white 96-well plates with a clear bottom and maintained at 37˚C and 5% CO_2 overnight for adherence. After the 4-h drug treatment, the drug-containing medium was discarded and replaced with 50 μl fresh medium. At each time point, 50 μl of the Caspase-Glo reaction reagent was added to the wells, the plate was shaken for 30 sec and was subsequently incubated for 30 min at room temperature. The luminescence of each well was analyzed using the SpectraMax iD3 Multi-Mode Microplate Reader. The luminescence values were normalized to the untreated control at each time point.

Treatment-related transcriptomic changes in PDAC cell lines. To record the transcriptional changes in PDAC cell lines upon identical total intracellular platinum challenge, a high-throughput reverse transcription-quantitative PCR (RT-qPCR) analysis was performed according to our previously published protocol using a Standard BioTools Inc. dynamic array on a BioMark™ system (19,20). After RNA isolation using the NucleoSpin® RNA Plus Kit (Machery-Nagel GmbH), 1 μg total RNA was reverse transcribed into cDNA with the qScript™ cDNA Synthesis Kit (Quantabio) according to the manufacturer's instructions. Specific target gene amplification was performed to obtain sufficient amounts of templates of the target genes for the subsequent high-throughput qPCR, followed by enzymatic digestion with *Escherichia coli* exonuclease I (New England BioLabs, Inc.) to remove unincorporated primers and dNTPs. For high-throughput qPCR, samples and primers [sequences of which are provided in a previous study (19)] were loaded onto a 96.96 Dynamic Array Integrated Fluidic Circuit (Standard BioTools Inc.), which was transferred into the BioMark HD System (Standard BioTools Inc.). qPCR (initial denaturation step at 95˚C for 10 min, followed by 12 cycles of 15 sec at 95˚C for denaturation, 4 min at 60˚C for annealing and elongation, and a final holding temperature of 4˚C) and melting curve analyses were performed as described previously (19). Evaluation and data analysis were performed with GenEx software (version 5.3.6.170; MultiD Analyses AB). For normalization, five reference genes were used [β-actin, β2-microglobulin (*β2MG*), glyceraldehyde-3-phosphate dehydrogenase, glucuronidase-β (*GUSB*) and hypoxanthine phosphoribosyltransferase 1]. Changes in the transcript levels of the target genes were displayed as fold change compared with the untreated control group by calculating relative quantities corresponding to the ΔΔCq method (21). The alterations in gene expression are shown as log2-fold changes with a value of 0 for the untreated control. This depiction was chosen as it enables a clear presentation of both induction (with the value 1 for two-fold enhancement) and repression (with the value-1 for reduction to 50%) of transcription.

Evaluating drug transporter expression levels in PDAC cell lines using RT-qPCR. Total RNA was isolated from untreated As-PC1 and Bx-PC3 cells using the GeneElute Mammalian Total RNA Miniprep Kit (Sigma-Aldrich; Merck KGaA) according to the manufacturer's instructions. cDNA was synthesized from total RNA using the RevertAid™ H Minus First Strand cDNA Synthesis Kit (Thermo Fisher Scientific, Inc.) according to the manufacturer's instructions. A random hexamer primer was used according to the manufacturer's instructions. The mRNA expression levels of *ABCC2, ATP7A, ATP7B, SLC22A1, SLC22A2, SLC22A3* and *SCL31A1* were quantified by qPCR [initial denaturation step at 95˚C for 15 min, followed by 40 cycles of 15 sec at 95˚C for strand melting, 30 sec at variable temperatures (see Table I) for primer annealing and 30 sec at 72˚C for elongation, followed by a melting curve analysis of 5 sec at 95˚C, 60 sec at 70˚C and 5 sec at 95˚C using a LightCycler® 480 (Roche Applied

Table I. Primer sequences.

Gene	Forward primer sequence, 5'-3'	Reverse primer sequence, 5'-3'	Primer annealing temperature, ˚C
ABCC2	ACAGAGGCTGGTGGCAACC	ACCATTACCTTGTCACTGTCCATGA	57
ATP7A	ATGATGAGCTGTGTGGCTTG	TGCCAACCTGAGAAGCAATAG	60
ATP7B	TACCCATTGCAGCAGGTGTC	ACTTGAGCTGCAGGGATGAG	57
SLC31A1	AGCTGGAGAAATGGCTGGAG	AGGTGAGGAAAGCTCAGCATC	63
SLC22A2	TCTACTCTGCCCTGGTTGAATTC	ATGCAGCCCAAGGGTAACG	57
SLC22A3	GGAGTTTCGCTCTGTTCAGG	GGAATGTGGACTGCCAAGTT	55
β2mg	CCAGCAGAGAATGGAAAGTC	CATGTCTCGATCCCACTTAAC	61
G6PDH	ATCGACCACTACCTGGGCAA	TCTGCATCACGTCCCGGA	61
GUSB	TTCACCAGGATCCACCTCTG	AGCACTCTCGTCGGTGACTG	61

β2mg, β2-microglobulin; *G6PDH*, glucose-6-phosphate-dehydrogenase; *GUSB*, glucuronidase-β.

Science) and the Quantifast SYBR Green Master mix (Qiagen GmbH) as described previously (22,23). The quantification of *SLC22A1* was performed using the Quantitect Hs_SLC22A1 kit (Qiagen GmbH). All other primer sequences were used as published previously (23,24) (Table I). Among a set of six housekeeping genes tested, glucose-6-phosphate-dehydrogenase, *GUSB* and *β2MG* were used for normalization. This approach minimizes the potential bias from correcting target gene expression levels to only one housekeeping gene (25). Accordingly, the Roche LightCycler 480 software determined the geometric mean Cq value of the three housekeeping genes by calculating the third root of [1st housekeeping gene x 2nd housekeeping gene x 3rd housekeeping gene], and the normalized expression level of the target gene was subsequently computed in line with the ΔCq method including an efficiency correction. Taken together, the data were analyzed as described previously (22). Three independent biological replicates with technical duplicates were performed for RT-qPCR.

RNA sequencing (RNAseq) data evaluation of hPDOs. RNA isolation, RT to cDNA, preparation of sequencing libraries and sequencing were performed as described previously (17). Briefly, total RNA was extracted from snap-frozen hPDO pellets using the AllPrep DNA/RNA/miRNA Universal Kit (Qiagen GmbH) and mRNA was purified using oligo(dT) beads. Poly(A)+ RNA was fragmented to 150 bp and converted to cDNA, which was end-repaired, adenylated on the 3-end, adapter-ligated and amplified with 15 cycles of PCR. Sequencing libraries were prepared using the Illumina TruSeq mRNA stranded kit (Illumina, Inc.) according the manufacturer's instructions. The final libraries were validated using Qubit (Invitrogen; Thermo Fisher Scientific, Inc.) and Tapetstation (Agilent Technologies, Inc.). Finally, 2x100 bp paired-end sequencing was performed on the Illumina NovaSeq 6000 (Illumina, Inc.) according to the manufacturer's protocol. At least 54 Mio reads per sample were generated.

Statistical analysis. Statistical analysis and generation of all figures were performed using GraphPad Prism 9 software (Version 9.0.0; Dotmatics). Differences between IC_{50} values [presented as the mean ± SD of four (cell lines) or three (hPDOs) independent experiments] were evaluated by unpaired Student's t-test. The statistical significance between the mean total intracellular platinum levels of the cell lines (treated with oxaliplatin or cisplatin) and the respective single experiments (AsPC-1 treated with 150 μM cisplatin; AsPC-1 treated with 176 μM oxaliplatin; BxPC-3 treated with 65 μM cisplatin; BxPC-3 treated with 150 μM oxaliplatin; presented as the mean ± SD of four to five independent experiments) was evaluated by non-parametric Kruskal-Wallis test and Dunn's post-hoc test, controlling for multiple testing. Differences in gene expression levels between drug-treated cell lines (presented as the mean ± SD of three independent experiments) were evaluated by a two-way ANOVA with Sidak's post-hoc test. $P<0.05$ was considered to indicate a statistically significant difference.

Results

Anti-proliferative pharmacodynamics of oxaliplatin. First, the anti-proliferative pharmacodynamics of oxaliplatin were evaluated in the cell lines (Fig. 1A and B). The IC_{50} of oxaliplatin in AsPC-1 cells was 88.8±45 μM, whereas it was 21±0.7 μM in BxPC-3 cells (P=0.02). Accordingly, AsPC-1 cells were 4.2-fold (±2.1) more oxaliplatin resistant than BxPC-3 cells. However, when anti-proliferative effects were normalized to total intracellular platinum levels, AsPC-1 cells (IC_{50}, 358±170 pg Pt/μg protein) remained 2.5-fold (±1.2) more resistant to oxaliplatin than BxPC-3 cells (IC_{50}, 142±12.8 pg Pt/μg protein; P=0.04), a non-significant decrease of resistance by 40% (P=0.21).

Second, the effects of oxaliplatin were tested on hPDOs (Fig. 1C and D). The IC_{50} of oxaliplatin in h19 cells was 684±153 μM, where it was 196±19.7 μM for h08 (P<0.029). Therefore, h19 was 3.5-fold (±0.8) more resistant to oxaliplatin than h08. After normalizing the anti-proliferative effects to total intracellular platinum levels, h19 (IC_{50} 779±205 pg Pt/μg protein) remained 2.8-fold (±0.7) more resistant than h08 (IC_{50}, 277±28.8 pg Pt/μg protein; P=0.04), a non-significant decrease of resistance by 20% (P=0.34).

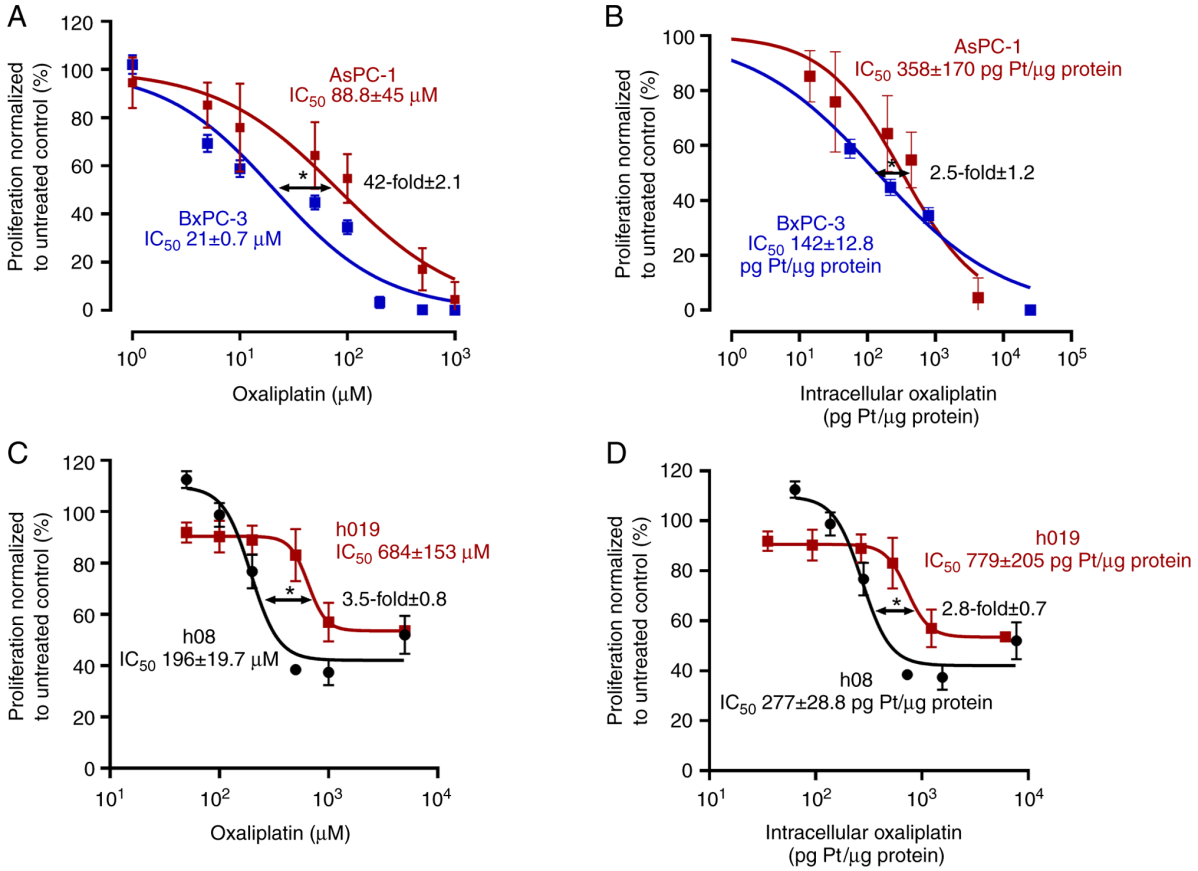

Figure 1. Anti-proliferative pharmacodynamics of oxaliplatin. Concentration-dependent proliferation inhibition in (A and B) AsPC-1 and BxPC-3 cells, and (C and D) h08 and h19 hPDOs, in response to (A and C) nominal extracellular exposure concentrations or (B and D) resulting total intracellular concentrations. Data are presented as the mean ± SD of four (cell lines) or three (hPDOs) independent experiments with technical octuplets each. Data were fitted to a sigmoidal dose-response curve with variable slope of the log-transformed data. *P<0.05. hPDOs, human patient-derived organoids.

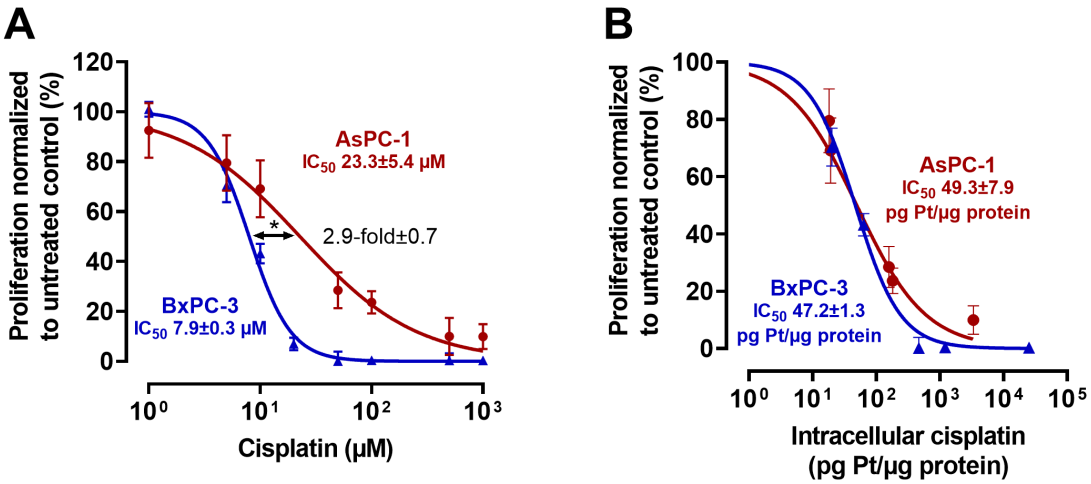

Figure 2. Anti-proliferative pharmacodynamics of the control drug cisplatin. Concentration-dependent proliferation inhibition in AsPC-1 and BxPC-3, in response to (A) nominal extracellular exposure concentrations or (B) resulting total intracellular concentrations. Data are presented as the mean ± SD of four independent experiments with technical octuplets each. Data were fitted to a sigmoidal dose-response curve with variable slope of the log-transformed data. *P<0.05.

To test for plausibility, the cell line experiments were repeated with cisplatin as a control drug (Fig. 2). The IC_{50} of cisplatin in AsPC-1 cells was 23.3±5.4 μM, whereas it was 7.9±0.3 μM in BxPC-3 cells (P<0.0013), a nominal resistance difference of 2.9-fold (±0.7). After normalization to total intracellular platinum levels, IC_{50} values were very similar (AsPC-1 IC_{50}, 49.3±7.9 pg Pt/μg protein; BxPC-3 IC_{50}, 47.2±1.3 pg Pt/μg protein), indicating a major role of drug uptake for cisplatin resistance.

Drug uptake. Drug uptake was calculated for two reasons. First, to again evaluate uptake characteristics. Second, to

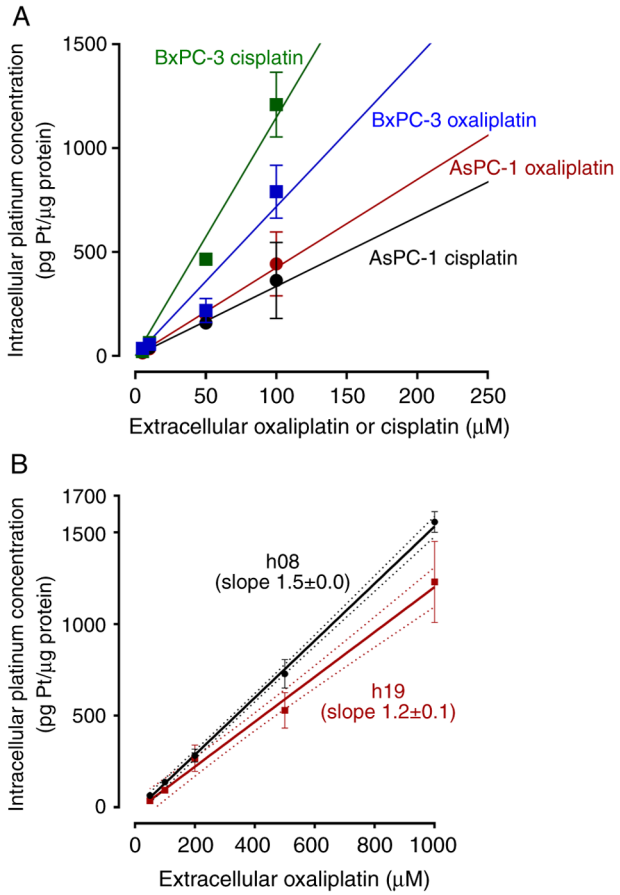

Figure 3. Uptake characteristics of platinum drugs. (A) Uptake of oxaliplatin or cisplatin into AsPC-1 and BxPC-3 cells, or (B) oxaliplatin uptake into h08 and h19 human patient-derived organoids. Data are presented as the mean ± SD of four independent experiments. Data were fitted to a linear regression, including the 95% confidence interval values for h08 and h19, which are presented as dotted lines.

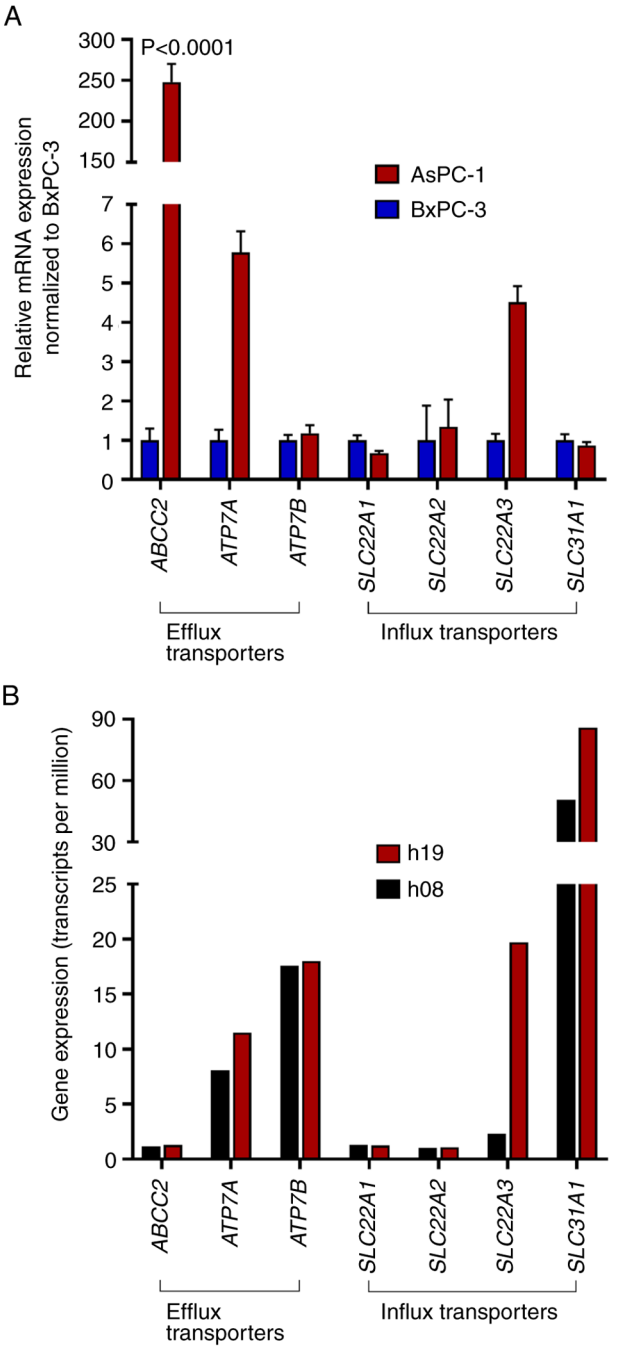

Figure 4. mRNA expression levels of major platinum drug transporters in untreated pancreatic ductal adenocarcinoma models. (A) Relative mRNA expression levels in AsPC-1 cells, normalized to the levels in BxPC-3 cells. Data are presented as the mean ± SD of three independent experiments with technical duplicates each (PCR runs). (B) mRNA expression levels in h19 and h08 human patient-derived organoids. The number of transcripts per million are shown, extracted from RNA sequencing data.

deduce extracellular concentrations that are needed to achieve the same intracellular drug concentrations during subsequent experiments. In the PDAC cell lines, uptake of oxaliplatin or cisplatin varied between the drugs and cell lines, as reflected by different slopes of the linear regression curves (Fig. 3A). In the hPDOs (Fig. 3B), the slopes for oxaliplatin uptake were significantly different (h08, slope 1.5±0.0; h19, slope 1.2±0.1; P=0.0003). By calculating the area-under-the-line, oxaliplatin uptake into h19 was 22% less than that into h08.

The mRNA expression levels of major platinum drug transporters were evaluated by PCR (cell lines) or were extracted from RNAseq data (hPDOs) (Fig. 4). Compared with in BxPC-3 cells, AsPC-1 cells expressed significantly higher levels of *ABCC2* (248±22-fold; P<0.0001). *ATP7A* (5.77±0.5-fold) and *SLC22A3* (4.5±0.4-fold) were also enhanced but the differences did not reach statistical significance (P>0.94). In the two hPDOs, there were also only minor differences in expression levels of platinum drug transporters, with one exception; *SLC22A3* was more highly expressed in h19 (19.7 transcripts per million) than in h08 (2.3 transcripts per million).

Caspase 3/7 assay. To assess caspase 3/7 activity in response to similar intracellular drug exposure, AsPC-1 cells were treated for 4 h with 150 μM cisplatin or 176 μM oxaliplatin, whereas BxPC-3 cells were treated with 65 μM cisplatin or 150 μM oxaliplatin. These treatments led to a mean total intracellular platinum concentration of 662±128 pg Pt/μg protein, with no statistical difference between any of the single experiments (Fig. 5A). Caspase 3/7 activity in BxPC-3 cells set in as early as 12 h post-treatment and peaked at 18 h (7-fold higher compared with the untreated control) without relevant differences between cells treated with oxaliplatin and cisplatin. By

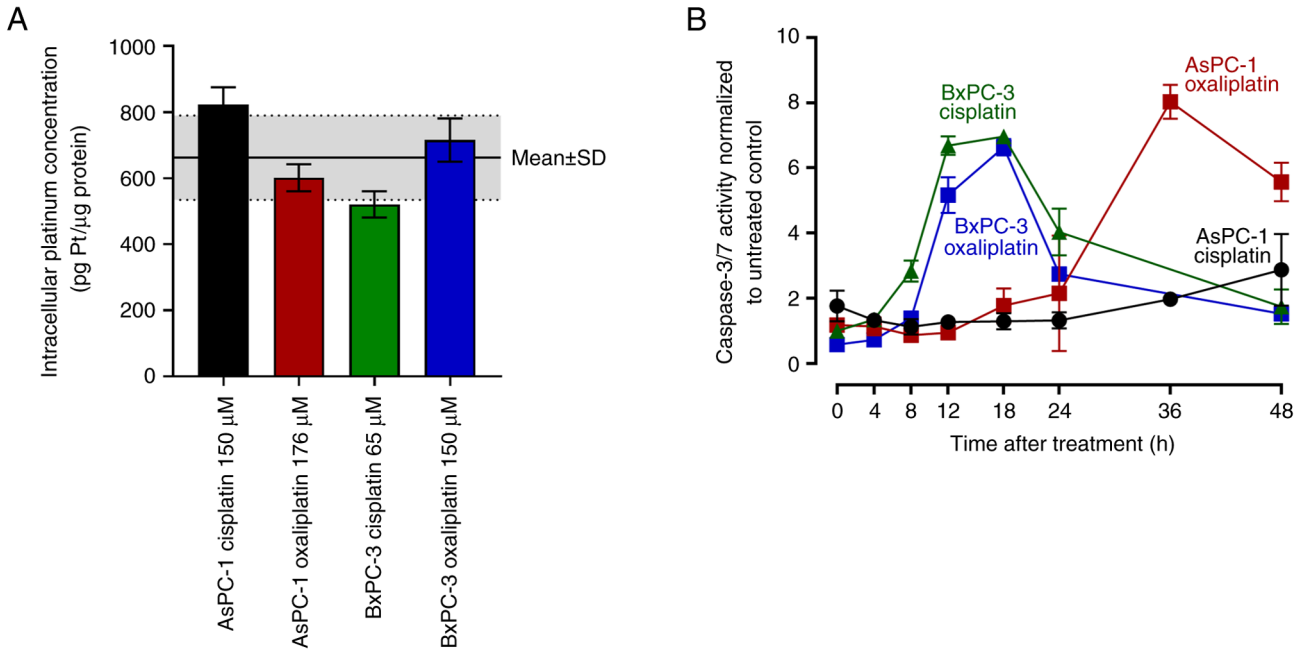

Figure 5. Caspase 3/7 activity upon similar platinum drug challenge. (A) Validation of similar total intracellular platinum concentrations in AsPC-1 and BxPC-3 cells after treatment with respective drug concentrations. Data are presented as the mean ± SD of four to five independent experiments. The black line represents the mean total intracellular platinum concentration of the four groups with the SD (gray area). (B) Kinetics of caspase 3/7 activity in cells after treatment with respective extracellular concentrations leading to similar total intracellular platinum concentrations. Data are presented as the mean ± SD of three to six independent experiments, normalized to the untreated control at the respective time point.

contrast, caspase 3/7 activity in AsPC-1 cells peaked 36 h after the end of oxaliplatin treatment (8-fold higher compared with the untreated control), whereas cisplatin treatment only weakly increased caspase 3/7 activity in AsPC-1 cells (3-fold 48 h post-treatment) (Fig. 5B).

Transcriptomics analysis of the response of PDAC cell lines to a cytotoxic threat. Cell lines were also screened for transcriptomic responses after exposure to the same intracellular drug levels as aforementioned. Treatment with oxaliplatin significantly enhanced the expression levels of genes implicated in inflammation. *IL-6* and *TNFα* were enhanced up to 2.5-fold in AsPC-1 cells and up to 7-fold in BxPC-3 cells (Figs. 6 and 7). Compared with in BxPC-3 cells, oxaliplatin treatment of AsPC-1 cells had a significantly weaker inducing effect on the pro-apoptotic *BBC3* (1.7-fold vs. 5-fold) and *PMAIP1* (2.5-fold vs. 6-fold), but a significantly stronger enhancing effect on the anti-apoptotic *Jun* (7-fold vs. 3-fold). Cisplatin (control drug) again enhanced *IL-6* (7-fold) and *TNFα* (29-fold) in BxPC-3 cells, whereas *IL-6* (1.12-fold) and *TNFα* (7.6-fold) inductions were rather weak in AsPC-1 cells. *BBC3* (1.1-fold vs. 3-fold) and *PMAIP1* (2.6-fold vs. 8-fold) were also more weakly induced in AsPC-1 cells than in BxPC-3 cells, and *Jun* was more strongly enhanced in AsPC-1 cells (6.5-fold) than in BxPC-3 cells (2-fold).

Gene expression levels in hPDOs. The genes evaluated in PDAC cell lines after drug treatment were also quantified in untreated hPDOs by extracting the expression levels from RNAseq data. Genes that were >2-fold higher expressed in h19 compared with h08 included *FTH1*, *GPX1*, *DDIT3*, *IL-8*, *VEGFA*, *BBC3*, *SIRT2*, *CDKN1A*, *XIAP* and *MT1X* (Fig. 8A). By contrast, 17 genes were >2-fold lower expressed (equals <50% relative expression) in h19, namely *GPX2*, *TIMP1*, *XRCC5*, *GSR*, *E2F1*, *DDB2*, *MSH2*, *TGFB*, *POLD1*, *LIG1*, *COL1A1*, *POLQ*, *FN1*, *ACTA2* and *VIM* (Fig. 8B).

Discussion

The present study aimed to assess which cellular factor contributes most to the oxaliplatin resistance phenotype in PDAC models. The investigation used two well-established PDAC cell lines, including AsPC-1 cells that have previously been shown to be oxaliplatin-resistant (26,27); the present study confirmed this by showing that the oxaliplatin IC_{50} in AsPC-1 cells was 4-fold higher than that in in BxPC-3 cells. From these data, however, it cannot be deduced as to whether this resistance originates from a lower drug uptake or if AsPC-1 cells possess molecular mechanisms that withstand the cytotoxic threat. Accordingly, drug uptake was evaluated and the recorded anti-proliferative effects were subsequently normalized to intracellular oxaliplatin concentrations. Notably, the resistance difference non-significantly decreased and remained at 2.5-fold. To substantiate this finding, two control experiments were performed. First, in contrast to oxaliplatin resistance, cisplatin resistance in AsPC-1 cells appeared to be more profoundly mediated by diminished drug uptake, given the near-perfect overlap of the concentration-response curves after normalization for intracellular cisplatin concentrations. Second, the oxaliplatin experiments were performed using two well-characterized hPDOs (17). In agreement with the cell lines, the oxaliplatin sensitivity of the hPDOs remained different despite identical intracellular oxaliplatin concentrations. Taken together, these findings suggested that poor

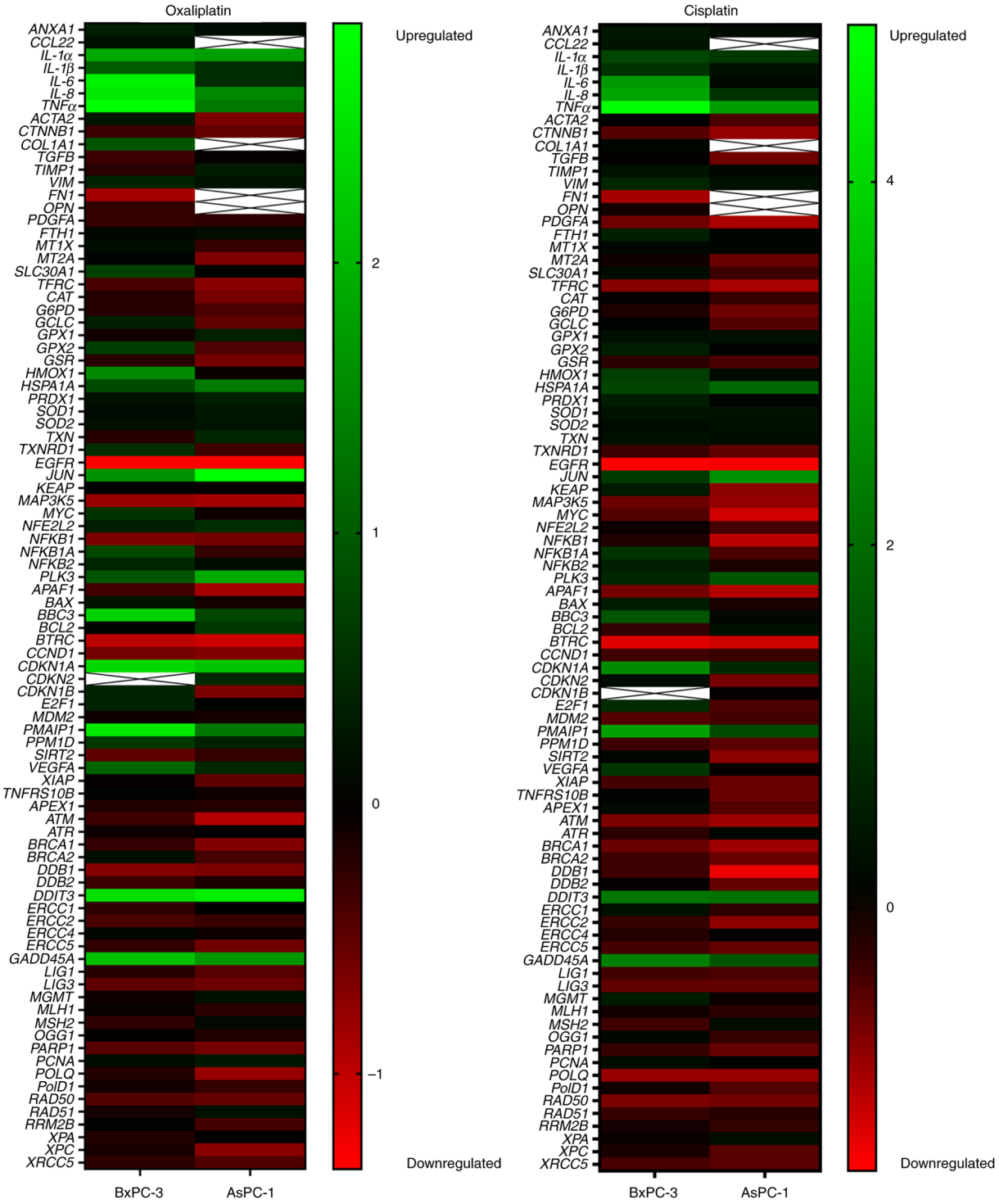

Figure 6. Treatment-related gene expression alterations. Heatmap of gene expression profiling of AsPC-1 and BxPC-3 cells after treatment with oxaliplatin or cisplatin concentrations that led to identical total intracellular platinum concentrations each. The log2 mean values of three independent experiments (with technical duplicates each) are shown, normalized to the untreated control set to 0. Missing values are indicated by white boxes.

oxaliplatin uptake may be of minor relevance for the resistance phenotype. This agrees with previous evaluations. A previous investigation on oxaliplatin-resistant colorectal cancer cell lines (generated by long-term oxaliplatin exposure) showed 5-fold (LoVo-Li cells) to 10-fold (LoVo-92 cells) higher oxaliplatin resistance than their parental counterparts, but with either only a 50% reduction of oxaliplatin accumulation (LoVo-92) or no alterations at all (LoVo-Li) compared with the parental counterparts prior to resistance induction (28). These findings indicate that high degrees of oxaliplatin resistance are not necessarily in line with drug accumulation. In the PDAC cell lines used in the present study, differences in the expression pattern of oxaliplatin transporters were also rather minor, with one exception. *ABCC2* (encoding the oxaliplatin efflux transporter MRP2) was 248-fold more highly expressed in AsPC-1 cells than in BxPC-3 cells. MRP2 has previously

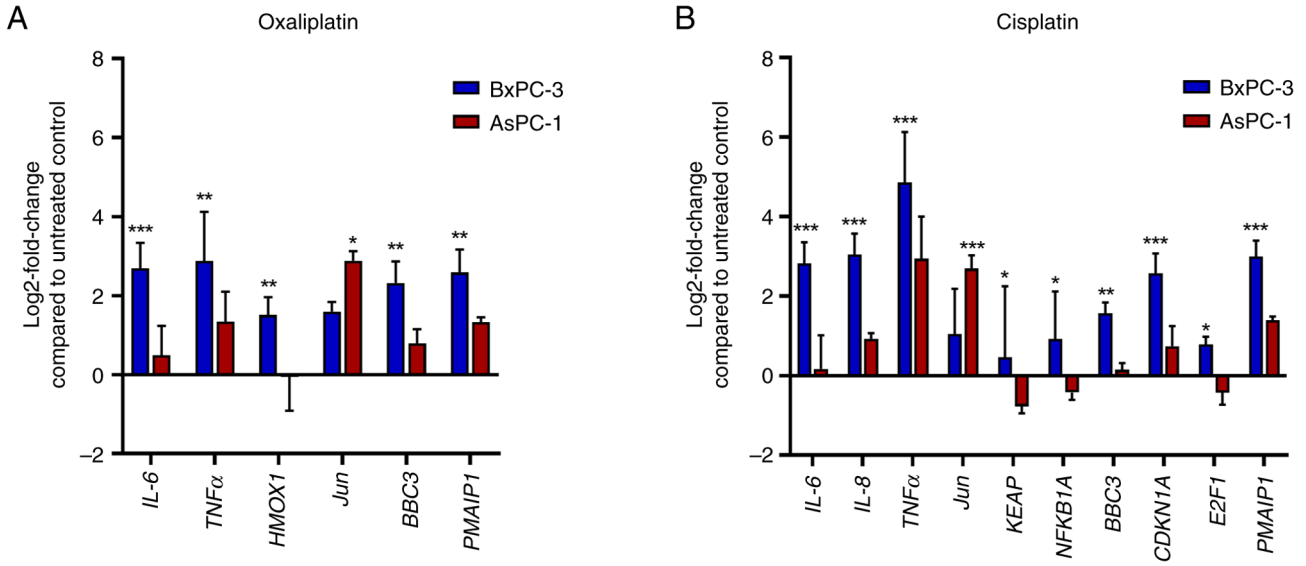

Figure 7. Treatment-related significant gene expression alterations. Statistically significant log2-fold changes of expression levels after exposure of AsPC-1 or BxPC-3 cells to (A) oxaliplatin or (B) cisplatin, which led to identical total intracellular platinum concentrations each. The log2 mean values ± SD of three independent experiments (with technical duplicates each) are shown, normalized to the untreated control set to 0. *P<0.01, **P<0.001, ***P<0.0001 indicates a significant difference of gene expression between AsPC-1 and BxPC-3 and is placed above the cell line with higher mRNA expression.

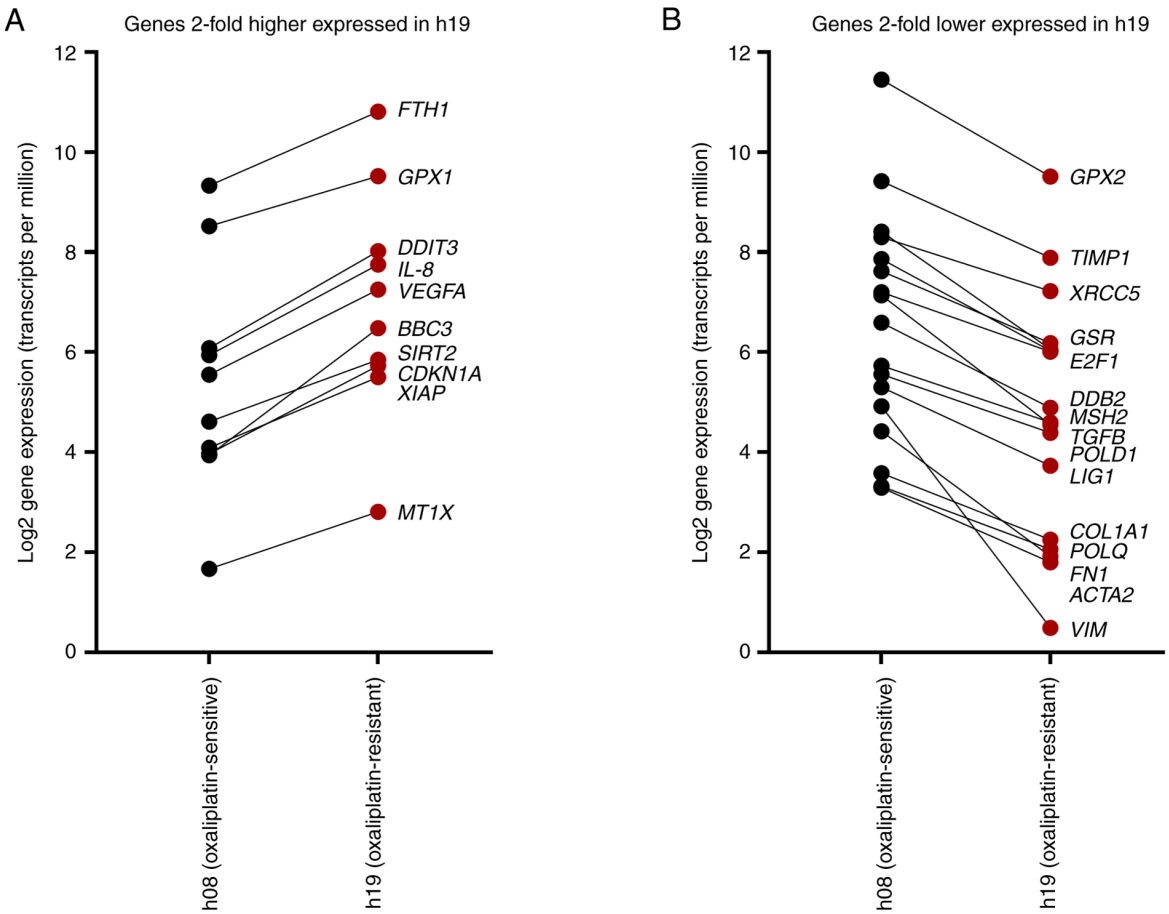

Figure 8. Relative gene expression levels in human patient-derived organoids. Genes with (A) 2-fold higher or (B) 2-fold lower expression levels in h19 (red) compared with h08 (black). Log2 gene expression is shown as transcripts per million.

been implicated in oxaliplatin resistance. For example, a knockdown of *ABCC2* by 50% also decreased oxaliplatin IC_{50} by 50-60% (29). Alternatively, transfection-mediated MRP2 overexpression has been shown to decrease platinum accumulation by 50% and to make cells 2-fold more oxaliplatin resistant (30). These findings however indicate that

even a genetically engineered cell model with artificially high transporter expression eventually only exhibits a 2-fold change in oxaliplatin potency, again questioning the relevance of drug uptake or transporter expression. Furthermore, both AsPC-1 cells and the h19 hPDO exhibited *SLC22A3* upregulation; this solute carrier is considered a biomarker for PDAC prognosis (31,32).

To scrutinize the molecular level of oxaliplatin resistance, the cell lines were treated with oxaliplatin (and cisplatin as a control) to obtain similar intracellular platinum levels (~662 pg Pt/μg protein) and subsequently underwent several experiments. Overall, the data indicated that AsPC-1 cells may handle the cytotoxic challenge differently than BxPC-3 cells. For example, caspase 3/7 activity was initiated later in AsPC-1 cells than that in BxPC-3 cells. Notably, the pro-apoptotic genes *BBC3* and *PMAIP1* were weakly enhanced in the oxaliplatin-resistant AsPC-1 cells, whereas the expression of the anti-apoptotic *Jun* was considerably boosted in AsPC-1 cells. Taken together, these findings suggest that PDAC may exhibit molecular switches that render cells resistant to pro-apoptotic signals or trigger sustained proliferation signals. This in turn also suggests these molecular switches being attractive pharmacological targets. However, most of the targeted therapeutics (including kinase inhibitors and monoclonal antibodies) have thus far disappointed in clinical assessments (1). Therefore, new targets are required. Among the known driver oncogenes in PDAC (including *CDKN2A*, *TP53* and *SMAD4*) that mediate sustained proliferation, mutated *KRAS* has been targeted in experimental and clinical investigations with somewhat promising results (2). Recently, a combined histone deacetylase/glycogen synthase kinase 3-β inhibitor (Metavert) has been shown to be efficacious against PDAC hPDOs, both alone, and particularly in combination with standard anti-PDAC drugs such as irinotecan (17). This shows that new agents may be developed, which can selectively address distinct pathogenic or resistance-mediating mechanisms.

The present study has weaknesses and strengths. Firstly, a broad set of resistance genes were evaluated at the mRNA level (such as *Jun*) and functional apoptosis initiation was assessed using a caspase 3/7 assay; however, these findings were not confirmed on the protein level (for example, by western blotting of select proteins) or by knockdown experiments. Accordingly, mass spectrometry-based profiling of the relevant proteins and their manipulation (such as knockdown) should be the next step in follow-up projects. Notably, the main limitation of the current study is that most of the data were obtained from established PDAC cell lines; therefore, general conclusions cannot be made for clinical PDAC. However, AsPC-1 and BxPC-3 cells are well-characterized PDAC models with precise information regarding their origin, differentiation, invasive capacity, angiogenic potential, tumorigenicity and genotype (33). Thus, these cell lines are considered meaningful models, which resemble important PDAC features. The present study provides important information on oxaliplatin uptake and the expression of drug transporters, and indicates that it is unlikely that the already observed oxaliplatin resistance in AsPC-1 cells (27) results from poor oxaliplatin accumulation, which was confirmed in hPDOs. Finally, the observations regarding delayed caspase 3/7 initiation and strong induction of *Jun* in AsPC-1 cells are in agreement with the p53-deficiency and apoptosis resistance already observed during the treatment of AsPC-1 cells with gemcitabine or interferon-γ (34,35).

In conclusion, oxaliplatin resistance in PDAC models may be highly linked to a poor apoptotic response (weak apoptosis initiation and poor induction of pro-apoptotic genes), while drug uptake seems to be of minor relevance.

Acknowledgements

The authors would like to thank Ms. Corina Mueller (Internal Medicine IX-Department of Clinical Pharmacology and Pharmacoepidemiology, Heidelberg University, Medical Faculty Heidelberg, Heidelberg University Hospital, Heidelberg, Germany), Ms. Jana Kuhn, Ms. Marlene Parsdorfer, Ms. Tatjana Lumpp and Ms. Sandra Stößer (all affiliated with Department of Food Chemistry and Toxicology, Karlsruhe Institute of Technology, Karlsruhe, Germany) for their valuable technical assistance.

Funding

No funding was received.

Availability of data and materials

The RNAseq raw data generated in the present study may be found in the European Genome-Phenome Archive under accession number EGAS00001007143 or at the following URL: https://ega-archive.org/studies/EGAS00001007143. The gene expression data (RT-qPCR) of the cell lines generated in the present study may be found in the Gene Expression Omnibus repository under accession number GSE308898 or at the following URL: https://www.ncbi.nlm.nih.gov/geo/query/acc.cgi?acc=GSE308898. The other data generated in the present study may be requested from the corresponding author.

Authors' contributions

HR, LT, BK, TP, KS, BK and DT designed the study, performed the experiments, analyzed the data and wrote the manuscript draft. JW, JB and JPN analyzed and interpreted the data and made manuscript revisions. DT and BK confirm the authenticity of all the raw data. All authors read and approved the final manuscript.

Ethics approval and consent to participate

Organoids were obtained during a previous study, which has been approved by the Ethics Committee of Heidelberg University (Heidelberg, Germany) for use in pancreatic cancer tissue and organoid generation (project nos. S-018/2020, S-708/2019 and S-083/2021). All patients provided written informed consent for use of their tissue and clinical data in accordance with The Declaration of Helsinki.

Patient consent for publication

Not applicable.

Competing interests

All authors declare that they have no competing interests.

References

1. Neoptolemos JP, Kleeff J, Michl P, Costello E, Greenhalf W and Palmer DH: Therapeutic developments in pancreatic cancer: Current and future perspectives. Nat Rev Gastroenterol Hepatol 15: 333-348, 2018.
2. Hu ZI and O'Reilly EM: Therapeutic developments in pancreatic cancer. Nat Rev Gastroenterol Hepatol 21: 7-24, 2024.
3. Gresham GK, Wells GA, Gill S, Cameron C and Jonker DJ: Chemotherapy regimens for advanced pancreatic cancer: A systematic review and network Meta-analysis. BMC Cancer 27: 471, 2014.
4. Chan K, Shah K, Lien K, Coyle D, Lam H and Ko YJ: A Bayesian meta-analysis of multiple treatment comparisons of systemic regimens for advanced pancreatic cancer. PLoS One 9: e108749, 2014.
5. Springfeld C, Jäger D, Büchler MW, Strobel O, Hackert T, Palmer DH and Neoptolemos JP: Chemotherapy for pancreatic cancer. Presse Med 48: e159-e174, 2019.
6. Martinez-Balibrea E, Martínez-Cardús A, Ginés A, Ruiz de Porras V, Moutinho C, Layos L, Manzano JL, Bugés C, Bystrup S, Esteller M and Abad A: Tumor-related molecular mechanisms of oxaliplatin resistance. Mol Cancer Ther 14: 1767-1776, 2015.
7. Burger H, Loos WJ, Eechoute K, Verweij J, Mathijssen RH and Wiemer EA: Drug transporters of Platinum-based anticancer agents and their clinical significance. Drug Resist Updat 14: 22-34, 2011.
8. Buß I, Hamacher A, Sarin N, Kassack MU and Kalayda GV: Relevance of copper transporter 1 and organic cation transporters 1-3 for oxaliplatin uptake and drug resistance in colorectal cancer cells. Metallomics 10: 414-425, 2018.
9. Martin LP, Hamilton TC and Schilder RJ: Platinum resistance: The role of DNA repair pathways. Clin Cancer Res 14: 1291-1295, 2008.
10. Grierson PM, Dodhiawala PB, Cheng Y, Chen TH, Khawar IA, Wei Q, Zhang D, Li L, Herndon J, Monahan JB, *et al*: The MK2/Hsp27 axis is a major survival mechanism for pancreatic ductal adenocarcinoma under genotoxic stress. Sci Transl Med 13: eabb5445, 2021.
11. Melisi D, Xia Q, Paradiso G, Ling J, Moccia T, Carbone C, Budillon A, Abbruzzese JL and Chiao PJ: Modulation of pancreatic cancer chemoresistance by inhibition of TAK1. J Natl Cancer Inst 103: 1190-1204, 2011.
12. Muniz VP, Askeland RW, Zhang X, Reed SM, Tompkins VS, Hagen J, McDowell BD, Button A, Smith BJ, Weydert JA, *et al*: RABL6A promotes oxaliplatin resistance in tumor cells and is a new marker of survival for resected pancreatic ductal adenocarcinoma patients. Genes Cancer 4: 273-284, 2013.
13. Jing W, Song N, Liu Y, Qu X, Hou K, Yang X and Che X: DNA methyltransferase 3a modulates chemosensitivity to gemcitabine and oxaliplatin via CHK1 and AKT in p53-deficient pancreatic cancer cells. Mol Med Rep 17: 117-124, 2018.
14. Pishvaian MJ, Biankin AV, Bailey P, Chang DK, Laheru D, Wolfgang CL and Brody JR: BRCA2 secondary mutation-mediated resistance to platinum and PARP Inhibitor-based therapy in pancreatic cancer. Br J Cancer 116: 1021-1026, 2017.
15. Lal S, Burkhart RA, Beeharry N, Bhattacharjee V, Londin ER, Cozzitorto JA, Romeo C, Jimbo M, Norris ZA, Yeo CJ, *et al*: HuR posttranscriptionally regulates WEE1: Implications for the DNA damage response in pancreatic cancer cells. Cancer Res 74: 1128-1140, 2014.
16. Xia R, Hu C, Ye Y, Zhang X, Li T, He R, Zheng S, Wen X and Chen R: HNF1A regulates oxaliplatin resistance in pancreatic cancer by targeting 53BP1. Int J Oncol 62: 45, 2023.
17. An J, Kurilov R, Peccerella T, Bergmann F, Edderkaoui M, Lim A, Zhou X, Pfütze K, Schulz A, Wolf S, *et al*: Metavert synergises with standard cytotoxics in human PDAC organoids and is associated with transcriptomic signatures of therapeutic response. Transl Oncol 49: 102109, 2024.
18. Peters T, Lindenmaier H, Haefeli WE and Weiss J: Interaction of the mitotic kinesin Eg5 inhibitor monastrol with P-glycoprotein. Naunyn Schmiedebergs Arch Pharmacol 372: 291-299, 2006.
19. Fischer BM, Neumann D, Piberger AL, Risnes SF, Köberle B and Hartwig A: Use of high-throughput RT-qPCR to assess modulations of gene expression profiles related to genomic stability and interactions by cadmium. Arch Toxicol 90: 2745-2761, 2016.
20. Rose F, Köberle B, Honnen S, Bay C, Burhenne J, Weiss J, Haefeli WE and Theile D: RNA is a pro-apoptotic target of cisplatin in cancer cell lines and C. elegans. Biomed Pharmacother 173: 116450, 2024.
21. Pfaffl MW: A new mathematical model for relative quantification in real-time RT-PCR. Nucleic Acids Res 29: e45, 2001.
22. Albermann N, Schmitz-Winnenthal FH, Z'graggen K, Volk C, Hoffmann MM, Haefeli WE and Weiss J: Expression of the drug transporters MDR1/ABCB1, MRP1/ABCC1, MRP2/ABCC2, BCRP/ABCG2, and PXR in peripheral blood mononuclear cells and their relationship with the expression in intestine and liver. Biochem Pharmacol 70: 949-958, 2005.
23. Weiss J, Herzog M and Haefeli WE: Differential modulation of the expression of important drug metabolising enzymes and transporters by endothelin-1 receptor antagonists ambrisentan and bosentan in vitro. Eur J Pharmacol 660: 298-304, 2011.
24. Theile D, Ketabi-Kiyanvash N, Herold-Mende C, Dyckhoff G, Efferth T, Bertholet V, Haefeli WE and Weiss J: Evaluation of drug transporters' significance for multidrug resistance in head and neck squamous cell carcinoma. Head Neck 33: 959-968, 2011.
25. Vandesompele J, De Preter K, Pattyn F, Poppe B, Van Roy N, De Paepe A and Speleman F: Accurate normalization of Real-time quantitative RT-PCR data by geometric averaging of multiple internal control genes. Genome Biol 3: RESEARCH0034, 2002.
26. Kuo SH, Yang SH, Wei MF, Lee HW, Tien YW, Cheng AL and Yeh KH: Contribution of nuclear BCL10 expression to tumor progression and poor prognosis of advanced and/or metastatic pancreatic ductal adenocarcinoma by activating NF-κB-related signaling. Cancer Cell Int 21: 436, 2021.
27. Lee JH, Lee SH, Lee SK, Choi JH, Lim S, Kim MS, Lee KM, Lee MW, Ku JL, Kim DH, *et al*: Antiproliferative activity of krukovine by regulating transmembrane protein 139 (TMEM139) in Oxaliplatin-resistant pancreatic cancer cells. Cancers (Basel) 15: 2642, 2023.
28. Noordhuis P, Laan AC, van de Born K, Honeywell RJ and Peters GJ: Coexisting molecular determinants of acquired oxaliplatin resistance in human colorectal and ovarian cancer cell lines. Int J Mol Sci 20: 3619, 2019.
29. Biswas R, Bugde P, He J, Merien F, Lu J, Liu DX, Myint K, Liu J, McKeage M and Li Y: Transport-mediated oxaliplatin resistance associated with endogenous overexpression of MRP2 in Caco-2 and PANC-1 Cells. Cancers (Basel) 11: 1330, 2019.
30. Myint K, Biswas R, Li Y, Jong N, Jamieson S, Liu J, Han C, Squire C, Merien F, Lu J, *et al*: Identification of MRP2 as a targetable factor limiting oxaliplatin accumulation and response in gastrointestinal cancer. Sci Rep 9: 2245, 2019.
31. Mohelnikova-Duchonova B, Brynychova V, Hlavac V, Kocik M, Oliverius M, Hlavsa J, Honsova E, Mazanec J, Kala Z, Melichar B and Soucek P: The association between the expression of solute carrier transporters and the prognosis of pancreatic cancer. Cancer Chemother Pharmacol 72: 669-682, 2013.
32. Cervenkova L, Vycital O, Bruha J, Rosendorf J, Palek R, Liska V, Daum O, Mohelnikova-Duchonova B and Soucek P: Protein expression of ABCC2 and SLC22A3 associates with prognosis of pancreatic adenocarcinoma. Sci Rep 9: 19782, 2019.
33. Deer EL, González-Hernández J, Coursen JD, Shea JE, Ngatia J, Scaife CL, Firpo MA and Mulvihill SJ: Phenotype and genotype of pancreatic cancer cell lines. Pancreas 39: 425-435, 2010.
34. Sugimoto H, Nakamura M, Yoda H, Hiraoka K, Shinohara K, Sang M, Fujiwara K, Shimozato O, Nagase H and Ozaki T: Silencing of RUNX2 enhances gemcitabine sensitivity of p53-deficient human pancreatic cancer AsPC-1 cells through the stimulation of TAp63-mediated cell death. Cell Death Dis 6: e1914, 2015.
35. Detjen KM, Farwig K, Welzel M, Wiedenmann B and Rosewicz S: Interferon gamma inhibits growth of human pancreatic carcinoma cells via caspase-1 dependent induction of apoptosis. Gut 49: 251-262, 2001.